

Modelling of impurity transport experiments at the Joint European Torus

H. Nordman¹, A. Skyman¹, P. Strand¹, C. Giroud², F. Jenko³, F. Merz³, M. Valisa⁴, P. Belo⁵, G. Corrigan², V. Naulin⁶, V. Parail², T. Tala⁷ and the JET-EFDA Contributors*.

JET-EFDA, Culham Science Centre, OX14 3DB, Abingdon, UK.

¹ Euratom-VR Association, Department of Radio and Space Science, Chalmers University of Technology, SE-412 96 Göteborg, Sweden.

² EURATOM/CCFE Association, Culham Science Centre, Abingdon, OX14 3DB UK.

³ Max-Planck-Institut für Plasmaphysik EURATOM-IPP, D-85748 Garching Germany.

⁴ Consorzio RFX – Associazione EURATOM-ENEA sulla Fusione, Padova, Italy.

⁵ EURATOM/IST Fusion Association, Instituto de Plasmas e Fusão Nuclear, Av. Rovisco Pais, 1049-001 Lisbon Portugal.

⁶ Association EURATOM/RISO-Technical University of Denmark, Roskilde, Denmark.

⁷ Association EURATOM-Tekes, VTT, P.O. Box 1000, FIN-02044 VTT, Finland.

* See the Appendix of F. Romanelli et al., Nucl. Fusion 49 (2009) 104006

Abstract

Impurity transport in JET is studied using interpretative analysis and predictive simulations of JET discharges. The simulations are based on transport models for Ion-Temperature-Gradient (ITG) mode and Trapped-Electron (TE) mode driven turbulence and neoclassical transport. The properties of the impurity transport coefficients obtained with fluid¹ as well as quasi-linear and nonlinear gyrokinetic simulations using the code GENE² are compared and discussed. In particular, the sign of the impurity convective velocity (pinch) and the scaling of the normalised impurity density peaking factor $-R\nabla n_z/n_z$ with impurity charge number is investigated. Predictive simulations of temperatures (T_e , $T_i=T_z$) and densities (n_e , n_z) are performed with the JETTO/SANCO core transport code.

The scaling of impurity transport with impurity charge Z is crucial for the performance and optimisation of a fusion reactor. In the present study, a set of dedicated JET impurity injection experiments³ are analysed. The impurities were injected by laser ablation (Ni) and gas injection (Ne, Ar) and the diffusivity D_Z and convective velocity V_Z were determined by matching spectroscopic data with predictive results obtained with the transport code UTC-SANCO.⁴

Fluid model

The Weiland multi-fluid model¹ has been used to describe the ITG/TE mode turbulence and the impurity species. The model equations consist of a set of fluid equations for the particle density, parallel velocity and temperature for each species, i.e. ions, trapped electrons and impurities. The impurity flux is calculated as $\Gamma_Z = \langle v_{\text{ExB}} \delta n_Z \rangle = -D_Z \nabla n_Z + n_Z V_Z$ where D_Z is the diffusivity and V_Z is the convective velocity. The convective velocity includes contributions from thermodiffusion, which scales as $V_Z \sim 1/Z \cdot R/L_{TZ}$ (usually outward for ITG-modes, inward for TE-modes), curvature (inward), and parallel impurity compression,⁵⁻⁶ $V_Z \sim Z/A_Z k_{\parallel}^2 \sim Z/(A_Z q^2)$, (usually inward for ITG-modes, outward for TE-modes). In the trace impurity approximation used here, the trace species is neglected in the quasi-neutrality condition and in this limit D_Z and V_Z are independent of ∇n_Z . In steady state the zero impurity flux condition $\Gamma_Z = 0$ gives the normalised impurity peaking factor $\text{PF} = -R \nabla n_Z / n_Z = -R V_Z / D_Z$ from the balance between the outward diffusion and convection.

Gyrokinetic model

The kinetic results have been obtained with the gyrokinetic code GENE.² The impurity flux is calculated for a few values of the impurity gradient ∇n_Z and then the diffusivity D_Z and convective velocity V_Z are obtained assuming a linear dependence between impurity flux and impurity density gradient. Most of the simulations have been done using the quasi-linear (QL) approximation in a low beta plasma equilibrium ($\beta \approx 10^{-3}$). The QL simulations calculate the flux from the dominant mode, which is the ITG mode for the cases considered. The nonlinear (NL) fluxtube simulations using GENE were performed with a box size of $L_x = L_y = 125 \rho_S$ with $n_x \times n_{ky} \times n_z = 96 \times 96 \times 32$ grid points in real space and $n_v \times n_{\mu} = 48 \times 12$ in velocity space.

Interpretative and predictive simulations

The anomalous impurity diffusivity D_Z , convective velocity V_Z , and normalised impurity peaking factor $\text{PF} = -R V_Z / D_Z$ are calculated from the background profiles of JET L-mode discharges #67730 and #67732. The main parameters are taken from L-mode discharge #67730 at $r/a = 0.5$ with $R/L_{Te} = 5.6$, $R/L_{Ti} = R/L_{TZ} = 5.6$, $f_i = 0.55$, $q = 2.4$, $s = 0.6$, $T_e/T_{i,z} = 0.98$, and $R/L_{ne} = 2.7$. The other parameters are $B = 3$ T, $R = 3$ m, $T_e = 1.55$ keV, $n_e = 1.84 \cdot 10^{19}$ m⁻³ and $P_{\text{NBI}} = 4.2$ MW. The simulations have been performed in a simple s - α equilibrium in the electrostatic limit.

The scaling of the normalised impurity density peaking factor with impurity charge Z , obtained with fluid, QL GENE and NL GENE simulations, is illustrated in Fig. 1. For the parameters used, the ITG mode is the dominant instability. The scaling with Z , with an increase in the peaking factor for increasing values of Z , is mainly a result of the thermodiffusive pinch (included here since $\nabla T_i = \nabla T_e$ is assumed), which is outward for ITG modes and scales as $1/Z$. The fluid and GENE results are in good agreement and show a saturation of the peaking factor for large values of Z ($Z > 10$) at a value slightly above the analytical fluid result ($PF=2$), which is obtained when neglecting parallel impurity compression.

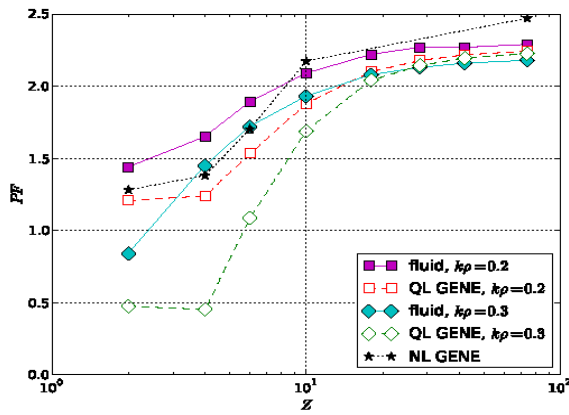


Fig. 1. Impurity peaking factor $PF = -R \nabla n_z / n_z$ versus Z for $Z \geq 2$ as obtained by Weiland fluid model and quasi-linear and nonlinear GENE simulations in the collisionless, electrostatic limit. Impurity mass $A_Z = 2Z$ is assumed. The parameters are taken from JET discharge #67730 at $r/a \approx 0.5$.

We have verified that the trace impurity approximation is adequate for the cases considered and that the results of Fig. 1 are rather insensitive to variations in other plasma parameters like e.g. collisionality and R/L_{ne} . The ratio D_z/χ_i shows a very weak scaling with Z with $D_z/\chi_i = 1.1$ (fluid) and $D_z/\chi_i \approx 1$ (NL GENE) for He.

A comparison with and experimental results for Ne, Ar and Ni show that the predicted values of D_z , V_z and D_z/χ_i and the Z -scaling are in reasonable agreement with experimental values.³ For Carbon however, the predicted peaking ($PF_C = 1.7-1.9$) is larger than the peaking obtained from the measured C profile which is flat or hollow at mid-radius. This may indicate that the contribution from thermodiffusion ($V_z \sim 1/Z \cdot R/L_{TZ}$), which is outward for ITG dominated cases, is larger than predicted by the present models.

The influence of sheared plasma rotation on the impurity peaking factor has been investigated. The ExB shearing rate $\gamma_E = dV_{ExB}/dr$ is treated as a parameter and the Waltz rule is applied with the linear growth rate γ_i replaced by $\gamma_{net} = \gamma_i - \gamma_E$ in the fluid transport coefficients. The impurity peaking factor versus the shearing parameter γ_E/γ_i is displayed in

Fig. 2 for the same parameters as in Fig. 1. The effective reduction of the ITG growth rate with ExB shearing is found to significantly reduce the peaking factors for low values of impurity charge Z . For He, a flux reversal, from an inward to an outward convective impurity velocity, is obtained for $\gamma_E/\gamma_i \approx 0.25$. The reduction of the ITG growth rate due to ExB shearing leads to a reduction of both the diffusive and convective fluxes. However, thermodiffusion is less affected resulting in a relative increase of its contribution compared to the other contributions to the impurity transport. Since the thermodiffusive flux is outward, the result is a reduction (or reversal) of the impurity peaking factor. The experimental value of the shearing parameter in #67730 at $r/a \approx 0.5$ is $\gamma_E/\gamma_i \approx 0.1$ and hence it does not significantly affect the predicted peaking factor for Carbon.

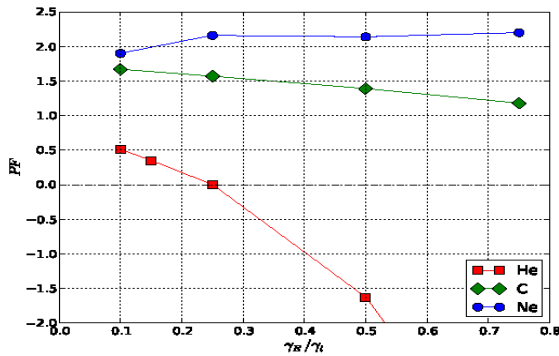


Fig. 2. Impurity peaking factor $-R\nabla n_Z/n_Z$ versus shearing parameter γ_E/γ_i . The parameters are taken from JET discharge #67730 at $r/a \approx 0.5$. The results are obtained with the fluid model.

Predictive simulations using JETTO/SANCO including neoclassical impurity transport from NCLASS show that for #67730 the predicted impurity profiles are consistent with the interpretative analysis for $Z \leq 18$. For larger Z -values, as well as in the inner core region ($\rho < 0.2$), neoclassical effects are dominant in the simulations resulting in substantially larger peaking factors than observed in the experiments.³

References

1. J. Weiland, Collective Modes in Inhomogeneous Plasmas, IoP 2000.
2. F. Jenko et al., Physics of Plasmas 7, 1904 (2000).
3. C. Giroud et al., 12th International Workshop on “H-mode Physics and Transport Barriers”, September 30-October 2 2009, Princeton, USA.
4. C. Giroud, et al, Nucl. Fusion 47, 313 (2007).
5. H. Nordman et al., Phys. Plasmas 14, 052303 (2007).
6. C. Angioni and A. G. Peeters, Phys. Rev. Lett. 96, 095003 (2006).